# FEM ANALYSES OF CUTTING OF ANISOTROPIC DENSELY COMPACTED AND SATURATED SAND

Jisong He[1], W.J. Vlasblom[2] and S. A. Miedema[3]

## ABSTRACT

The literature studies show that until now, the existing investigations on the cutting of densely compacted and saturated sand are involved only in the range of isotropic soil with regard to permeability. The permeability of sand is one of the most important parameters in saturated sand cutting. The properties of the isotropic soil that are responsible for the resistance to flow are independent of the direction. However, in many soil deposits the resistance to flow in the vertical direction is considerably larger than the resistance to horizontal flow, due to the presence of the layered structure in the soil, generated by its geological history. It is necessary to investigate the cutting of anisotropic densely compacted and saturated sand.

This paper builds up a mathematical modeling of the cutting of anisotropic densely compacted and saturated sand and performs finite element analysis of saturated sand cutting with the ratio $k_h / k_v$ =1, 2, 4, 6, 8, 10 of permeability of soil in the horizontal direction to that in the vertical direction, and with various shear angles ranging from 15 degree to 35 degree.

The results show the cutting forces required for anisotropic densely compacted and saturated sand will increase with the ratio $k_h / k_v$. The cutting force for a soil with $k_h / k_v$ =10 is about 18 % larger than that of an isotropic sand

**Keywords:** finite element method, soil, dilatancy, pore water pressure, permeability,

## INTRODUCTION

When the cutting of soil is investigated, the homogeneous soil has been almost all assumed in order to simplify the problems (Os, 1976 and 1987; Miedema, 1985, 1987). However, generally speaking, soil in the real world is anisotropic. What is the difference when the anisotropic soil is used instead of homogeneous soil? The cutting of saturated anisotropic soil is a very complicated subject because it has effects on the strength and permeability and other parameters of soil. However, dilatancy is more important in the cutting of saturated sand. In the paper the effects of anisotropic permeability of densely compacted and saturated sand on the cutting forces will be discussed, because pore water pressure plays a most important role in the cutting of densely compacted and saturated sand and permeability has strong effects on the change of the pore water pressure.

## MATHEMATICAL MODEL OF CUTTING OF ANISOTROPIC SATURATED SOIL

The literature studies show that the investigations on the cutting of densely compacted and saturated sand are involved in the range of isotropic soil with regard to permeability. The properties of this type of the soil that are responsible for the resistance to flow are independent of the direction. However, in many soil deposits the resistance to flow in the vertical direction is considerably larger than the resistance to horizontal flow, due to the presence of a layered structure in the soil, generated by its geological history. Only the two-dimensional cutting of anisotropic soil is considered in this paper.

For two-dimensional anisotropic soil, Darcy's law can be expressed:

[1] Engineer, HL engineering company, Oeverwallaan 37, Den Haag, 2498 BV, The Netherlands, T: +31-15-2573812, Fax: +31-15-2573812, Email. jisonghe@hotmail.nl

[2] Professor, Delft University of Technology, Faculty of Mechanical Engineering, Mekelweg 2,2628 CD Delft, The Netherlands, T: +31-15-2783937,Fax: +31-15-2781397, Email. W.J.Vlasblom@wbmt.tudelft.nl

[3] Dr. Ir, Delft University of Technology, Faculty of Mechanical Engineering, Mekelweg 2,2628 CD Delft, The Netherlands T: +31-15-2788359,Fax: +31-15-2781397, Email. S.A.Miedema@wbmt.tudelft.nl

$$\begin{pmatrix} q_x \\ q_y \end{pmatrix} = \begin{bmatrix} -k_{xx} & -k_{xy} \\ -k_{xy} & -k_{yy} \end{bmatrix} \begin{pmatrix} \dfrac{\partial p}{\partial x} \\ \dfrac{\partial p}{\partial y} \end{pmatrix} \tag{1}$$

This matrix expresses the most general linear relationship between the specific discharge vector and the gradient of the pore pressure. The permeability matrix is a symmetric matrix, so there exist two mutually orthogonal directions, the so-called principal directions of permeability, in which the cross-components disappear. When the soil is orthogonal, equation 1 becomes:

$$\begin{pmatrix} q_x \\ q_y \end{pmatrix} = \begin{bmatrix} -k_{xx} & 0 \\ 0 & -k_{yy} \end{bmatrix} \begin{pmatrix} \dfrac{\partial p}{\partial x} \\ \dfrac{\partial p}{\partial y} \end{pmatrix} \tag{2}$$

Physically speaking, this means that a gradient of the pore water pressure in one of these directions leads to a flow in the same direction. The soil to be cut consists of two orthogonal pore channels with different cross sections and with different resistances, see Figure 1. The principal directions coincide with the direction of the pore channels

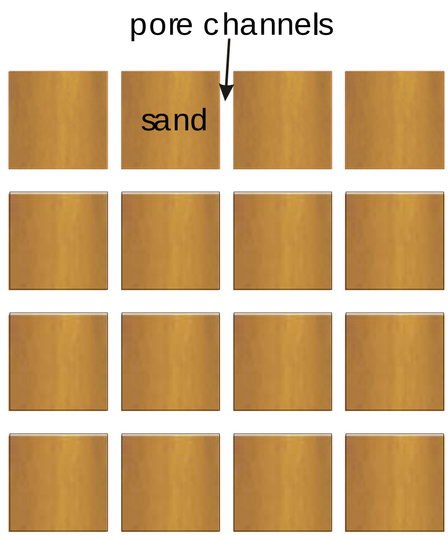


**Figure 1. Two-dimensional model**

If the pore channels in the x-direction are wider than those in the y-direction, the permeability $k_{xx}$ will be greater than $k_{yy}$. Now we calculate the values of permeability in another coordinate system $(\xi, \eta)$ which rotates an angle α with the coordinate system $(x, y)$. There is a relationship between these two coordinate systems:

$$\begin{pmatrix} \xi \\ \eta \end{pmatrix} = \begin{bmatrix} \cos\alpha & \sin\alpha \\ -\sin\alpha & \cos\alpha \end{bmatrix} \begin{pmatrix} x \\ y \end{pmatrix} \tag{3}$$

A vector q with components $q_x$ *and* $q_y$ can be decomposed into components $q_\xi$ *and* $q_\eta$:

$$\begin{pmatrix} q_\xi \\ q_\eta \end{pmatrix} = \begin{bmatrix} \cos\alpha & \sin\alpha \\ -\sin\alpha & \cos\alpha \end{bmatrix} \begin{pmatrix} q_x \\ q_y \end{pmatrix} \tag{4}$$

Substituting equation 1 into the matrix above, one obtains:

$$\begin{pmatrix} q_\xi \\ q_\eta \end{pmatrix} = \begin{bmatrix} \cos\alpha & \sin\alpha \\ -\sin\alpha & \cos\alpha \end{bmatrix} \begin{bmatrix} -k_{xx} & -k_{xy} \\ -k_{xy} & -k_{yy} \end{bmatrix} \begin{pmatrix} \dfrac{\partial p}{\partial x} \\ \dfrac{\partial p}{\partial y} \end{pmatrix} \tag{5}$$

The partial derivative $\dfrac{\partial p}{\partial x}$ *and* $\dfrac{\partial p}{\partial y}$ can be expressed by $\dfrac{\partial p}{\partial \xi}$, *and* $\dfrac{\partial p}{\partial \eta}$ with equation (3):

$$\begin{pmatrix} \dfrac{\partial p}{\partial x} \\ \dfrac{\partial p}{\partial y} \end{pmatrix} = \begin{pmatrix} \dfrac{\partial p}{\partial \xi}\dfrac{\partial \xi}{\partial x} + \dfrac{\partial p}{\partial \eta}\dfrac{\partial \eta}{\partial x} \\ \dfrac{\partial p}{\partial \xi}\dfrac{\partial \xi}{\partial y} + \dfrac{\partial p}{\partial \eta}\dfrac{\partial \eta}{\partial y} \end{pmatrix} = \begin{bmatrix} \cos\alpha & -\sin\alpha \\ \sin\alpha & \cos\alpha \end{bmatrix} \begin{pmatrix} \dfrac{\partial p}{\partial \xi} \\ \dfrac{\partial p}{\partial \eta} \end{pmatrix} \tag{6}$$

Substituting the equation above into equation 5, one obtains:

$$\begin{pmatrix} q_\xi \\ q_\eta \end{pmatrix} = \begin{bmatrix} \cos\alpha & \sin\alpha \\ -\sin\alpha & \cos\alpha \end{bmatrix} \begin{bmatrix} -k_{xx} & 0 \\ 0 & -k_{yy} \end{bmatrix} \begin{bmatrix} \cos\alpha & -\sin\alpha \\ \sin\alpha & \cos\alpha \end{bmatrix} \begin{pmatrix} \dfrac{\partial p}{\partial \xi} \\ \dfrac{\partial p}{\partial \eta} \end{pmatrix} \tag{7}$$

The specific charge $q_{\xi,}\ q_\eta$ can also be written as:

$$\begin{pmatrix} q_\xi \\ q_\eta \end{pmatrix} = \begin{bmatrix} -k_{\xi\xi} & -k_{\xi\eta} \\ -k_{\xi\eta} & -k_{\eta\eta} \end{bmatrix} \begin{pmatrix} \dfrac{\partial p}{\partial \xi} \\ \dfrac{\partial p}{\partial \eta} \end{pmatrix} \tag{8}$$

From the above two equations, one obtains:

$$\begin{bmatrix} -k_{\xi\xi} & -k_{\xi\eta} \\ -k_{\xi\eta} & -k_{\eta\eta} \end{bmatrix} = \begin{bmatrix} \cos\alpha & \sin\alpha \\ -\sin\alpha & \cos\alpha \end{bmatrix} \begin{bmatrix} -k_{xx} & 0 \\ 0 & -k_{yy} \end{bmatrix} \begin{bmatrix} \cos\alpha & -\sin\alpha \\ \sin\alpha & \cos\alpha \end{bmatrix} \tag{9}$$

They are expanded as:

$$\begin{aligned} k_{\xi\xi} &= k_{xx}\cos^2\alpha + k_{yy}\sin^2\alpha = \frac{k_{xx}+k_{yy}}{2} - \frac{k_{yy}-k_{xx}}{2}\cos 2\alpha \\ k_{\eta\eta} &= k_{yy}\cos^2\alpha + k_{xx}\sin^2\alpha = \frac{k_{xx}+k_{yy}}{2} + \frac{k_{yy}-k_{xx}}{2}\cos 2\alpha \\ k_{\xi\eta} &= (k_{yy}-k_{xx})\sin\alpha\cos\alpha = \frac{k_{yy}-k_{xx}}{2}\sin 2\alpha \end{aligned} \tag{10}$$

The equation above indicates when the soil is isotropic namely $k_{xx} = k_{yy}$, or when the coordinate system $(\xi,\eta)$ coincides with coordinate system (x, y), $k_{\xi\eta}$ =0. The equation above describes a general flow using the coordinate system ( $(\xi,\eta)$ . It shows that a gradient of pore water pressure in $\xi$ direction not only leads to a flow in its direction but also to a flow in $\eta$ -direction.

The channels in x-direction will physically transport much more water than the narrow channels in y-direction because $k_{xx}$ is greater than $k_{yy}$ . In general the resultant flow will always have a tendency towards the most permeable direction. The anisotropic law should be of the form of equation 3. In engineering practice the orthogonal situation is usually acceptable to distinguish only between the permeability in vertical direction and the one in horizontal direction, assuming that this difference has been created during the geological process of deposition of the soil. It is assumed that the x, y directions of permeability are its principal directions.

In the cutting of saturated sand, storage equation is one of the basic equations, which is from Biot's theory of consolidation (Biot, 1941). This equation expresses that volumetric deformations of the soil must be accompanied by a compression or expulsion of the pore water. Storage equation of soil cutting is:

$$\frac{\partial e}{\partial t} = -(\frac{\partial q_x}{\partial x} + \frac{\partial q_y}{\partial y}) \tag{11}$$

The volumetric strain rate $\partial e / \partial t$ can be expressed in the change of porosity, using the assumption that the soil particles are incompressible.

$$\frac{\partial e}{\partial t} = \frac{1}{1-n}\frac{\partial n}{\partial t} \tag{12}$$

Substituting the equation above and equation 1 into equation 13, one obtains:

$$-(\frac{\partial q_x}{\partial x} + \frac{\partial q_y}{\partial y}) = \frac{1}{1-n}\frac{\partial n}{\partial t} \tag{13}$$

$$-\frac{1}{\rho_w g}(k_{xx}\frac{\partial^2 p}{\partial x^2} + k_{yy}\frac{\partial^2 p}{\partial y^2} + 2k_{xy}\frac{\partial^2 p}{\partial x \partial y}) = \frac{1}{1-n}\frac{\partial n}{\partial t} \tag{14}$$

In continuous cutting process, it is convenient to introduce a moving coordinate system, with

$$\zeta = x - v_c t \tag{15}$$

Where $v_c$ is the velocity of the cutting blade.

Equation 14 becomes:

$$-\frac{1}{\rho_w g}(k_{\zeta\zeta}\frac{\partial^2 p}{\partial \zeta^2} + k_{yy}\frac{\partial^2 p}{\partial y^2} + 2k_{\zeta y}\frac{\partial^2 p}{\partial \zeta \partial y}) = \frac{v_c}{1-n}\frac{\partial n}{\partial \zeta} \tag{16}$$

For the saturated soil cutting, the soil failure is considered to occur in shear areas R, so that the following equations describe the cutting problem:

$$\begin{cases} \frac{1}{\rho_w g}(k_{xx}\frac{\partial^2 p}{\partial x^2} + k_{yy}\frac{\partial^2 p}{\partial y^2} + 2k_{xy}\frac{\partial^2 p}{\partial x \partial y}) = 0 & \text{(x,y)} \notin \text{R} \\ \frac{1}{\rho_w g}(k_{xx}\frac{\partial^2 p}{\partial x^2} + k_{yy}\frac{\partial^2 p}{\partial y^2} + 2k_{xy}\frac{\partial^2 p}{\partial x \partial y}) = \frac{v_c}{1-n}\frac{\Delta n}{\Delta x} & \text{(x,y)} \in \text{R} \end{cases} \tag{17}$$

When coordinate system (x, y) is the principal coordinate system of the permeability, the equations above become:

$$\begin{cases} \frac{1}{\rho_w g}(k_{xx}\frac{\partial^2 p}{\partial x^2} + k_{yy}\frac{\partial^2 p}{\partial y^2}) = 0 & \text{(x,y)} \notin \text{R} \\ \frac{1}{\rho_w g}(k_{xx}\frac{\partial^2 p}{\partial x^2} + k_{yy}\frac{\partial^2 p}{\partial y^2}) = \frac{v_c}{1-n}\frac{\Delta n}{\Delta x} & \text{(x,y)} \in \text{R} \end{cases} \tag{18}$$

Using the following relationships, one can make the dimensionless of the equation 18.

$$\begin{cases} q^1 = \dfrac{q}{\rho_w \cdot g \cdot e \cdot v_c \cdot h / k_{\max}} \\ x' = x/h \\ y' = y/h \end{cases} \tag{19}$$

It can be rewritten as:

$$\begin{cases} \dfrac{k_{xx}}{k_{\max}} \dfrac{\partial^2 p^1}{\partial x'^2} + \dfrac{k_{yy}}{k_{\max}} \dfrac{\partial^2 p^1}{\partial y'^2} = 0 & (x', y') \notin R \\ \dfrac{k_{xx}}{k_{\max}} \dfrac{\partial^2 p^1}{\partial x'^2} + \dfrac{k_{yy}}{k_{\max}} \dfrac{\partial^2 p^1}{\partial y'^2} = \dfrac{h}{\Delta x} & (x', y') \in R \end{cases} \tag{20}$$

**MODELING AND ANALYSES OF FEM**

Because the calculation formulae of the cutting forces for the anisotropic saturated soil are the same as those for isotropic saturated soil. Only the effects of the pore water pressure are considered because of the anisotropic permeability of the soil. Figure 2 is a FEM model of the cutting of anisotropic saturated soil. In the model, the permeability of the initial saturated soil is $k_{xx}$ =0.25 and $k_{xx} / k_{yy}$ = 1, 2, 4, 6, 8, 10. The permeability of the cut soil in the rigid wedge is isotropic: $k_{xx} = k_{yy} = k_{\max} = 1$. The cutting angle of the blade is 60 degree; shearing angle β is respectively 15, 20, 25, 30 and 35 degrees. Ratio of the vertical height of the blade to the cutting depth is 3.

The results of the calculations of dimensionless average pore pressures distributed both on the cutting blade (p-blade) and on the shear surface (p-shear), and of horizontal-cutting forces for different soil with internal friction angles of 20 to 45 degrees are listed in table 1. Because the calculations are dimensionless, the following equation is valid:

$$p = (\rho_w \cdot g \cdot e \cdot v_c \cdot h / k_{\max}) \cdot p_{cal} \tag{21}$$

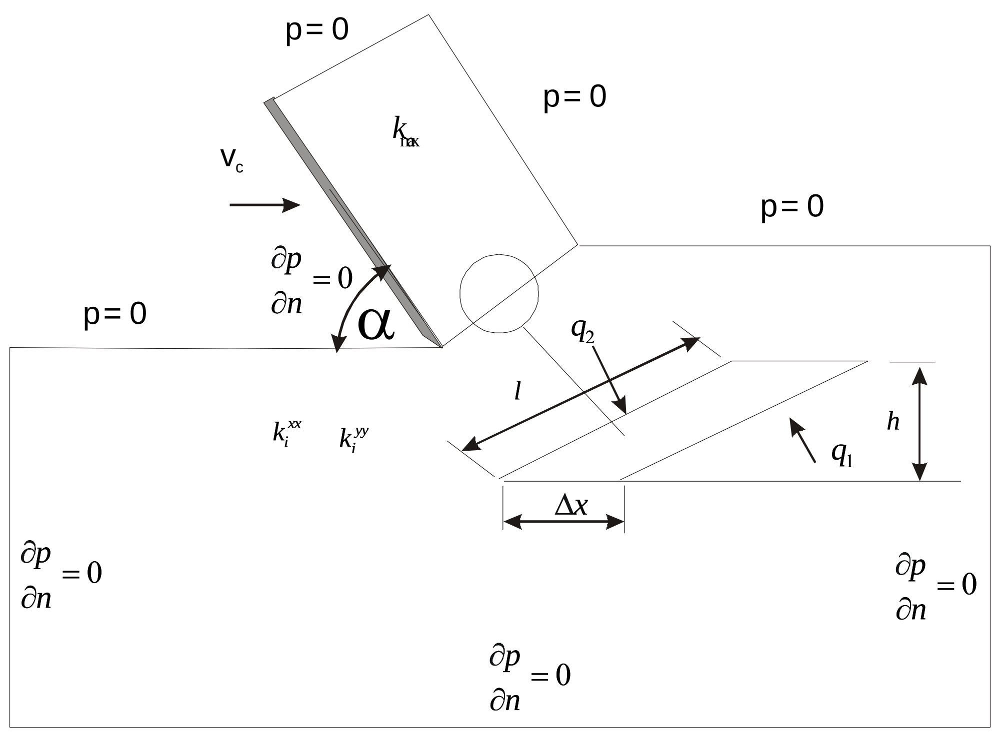


**Figure 2: FEM model of saturated sand cutting**

**Table 1: Results of FEM analyses of cutting of anisotropic saturated soil**

| $\beta$ | $k_{xx} / k_{yy}$ | Pore pressure | | Fh | | | | | |
|---|---|---|---|---|---|---|---|---|---|
| | | p-Blade | p-shear | $\varphi$ =20º | $\varphi$ =25º | $\varphi$ =30º | $\varphi$ =35º | $\varphi$ =30º | $\varphi$ =45º |
| 15 | 1 | 0.1600 | 0.3519 | 0.4035 | 0.5411 | 0.7107 | 0.9308 | 1.2359 | 1.6977 |
| | 2 | 0.1724 | 0.3739 | 0.4290 | 0.5753 | 0.7556 | 0.9898 | 1.3143 | 1.8056 |
| | 4 | 0.1818 | 0.3905 | 0.4484 | 0.6013 | 0.7898 | 1.0347 | 1.3739 | 1.8875 |
| | 6 | 0.1860 | 0.3981 | 0.4572 | 0.6131 | 0.8053 | 1.0550 | 1.4009 | 1.9247 |
| | 8 | 0.1884 | 0.4026 | 0.4624 | 0.6201 | 0.8146 | 1.0671 | 1.4170 | 1.9468 |
| | 10 | 0.1901 | 0.4057 | 0.4660 | 0.6249 | 0.8209 | 1.0754 | 1.4280 | 1.9619 |
| 20 | 1 | 0.1776 | 0.3834 | 0.3530 | 0.4813 | 0.6445 | 0.8646 | 1.1852 | 1.7080 |
| | 2 | 0.1917 | 0.4088 | 0.3768 | 0.5137 | 0.6880 | 0.9230 | 1.2653 | 1.8236 |
| | 4 | 0.2023 | 0.4282 | 0.3949 | 0.5384 | 0.7210 | 0.9674 | 1.3263 | 1.9115 |
| | 6 | 0.2071 | 0.4370 | 0.4031 | 0.5496 | 0.7361 | 0.9876 | 1.3540 | 1.9514 |
| | 8 | 0.2100 | 0.4423 | 0.4080 | 0.5563 | 0.7451 | 0.9997 | 1.3706 | 1.9754 |
| | 10 | 0.2119 | 0.4459 | 0.4114 | 0.5609 | 0.7512 | 1.0079 | 1.3819 | 1.9918 |
| 25 | 1 | 0.1852 | 0.4073 | 0.3247 | 0.4505 | 0.6161 | 0.8496 | 1.2115 | 1.8636 |
| | 2 | 0.1998 | 0.4352 | 0.3473 | 0.4818 | 0.6590 | 0.9088 | 1.2961 | 1.9937 |
| | 4 | 0.2110 | 0.4565 | 0.3645 | 0.5057 | 0.6917 | 0.9539 | 1.3605 | 2.0929 |
| | 6 | 0.2161 | 0.4662 | 0.3724 | 0.5167 | 0.7067 | 0.9746 | 1.3900 | 2.1383 |
| | 8 | 0.2191 | 0.4721 | 0.3771 | 0.5233 | 0.7158 | 0.9871 | 1.4078 | 2.1657 |
| | 10 | 0.2212 | 0.4762 | 0.3804 | 0.5278 | 0.7220 | 0.9957 | 1.4201 | 2.1847 |
| 30 | 1 | 0.1876 | 0.4272 | 0.3104 | 0.4389 | 0.6148 | 0.8764 | 1.3162 | 2.2320 |
| | 2 | 0.2024 | 0.4569 | 0.3323 | 0.4699 | 0.6583 | 0.9385 | 1.4094 | 2.3902 |
| | 4 | 0.2136 | 0.4796 | 0.3491 | 0.4936 | 0.6916 | 0.9859 | 1.4808 | 2.5113 |
| | 6 | 0.2188 | 0.4901 | 0.3569 | 0.5046 | 0.7070 | 1.0079 | 1.5137 | 2.5672 |
| | 8 | 0.2220 | 0.4965 | 0.3616 | 0.5113 | 0.7163 | 1.0213 | 1.5339 | 2.6013 |
| | 10 | 0.2241 | 0.5010 | 0.3649 | 0.5159 | 0.7229 | 1.0305 | 1.5478 | 2.6250 |
| 35 | 1 | 0.1880 | 0.4450 | 0.3068 | 0.4430 | 0.6385 | 0.9495 | 1.5340 | 3.0769 |
| | 2 | 0.2027 | 0.4764 | 0.3287 | 0.4747 | 0.6843 | 1.0176 | 1.6440 | 3.2977 |
| | 4 | 0.2140 | 0.5006 | 0.3457 | 0.4992 | 0.7196 | 1.0701 | 1.7289 | 3.4681 |
| | 6 | 0.2193 | 0.5119 | 0.3536 | 0.5106 | 0.7361 | 1.0946 | 1.7686 | 3.5477 |
| | 8 | 0.2225 | 0.5189 | 0.3585 | 0.5177 | 0.7462 | 1.1097 | 1.7930 | 3.5968 |
| | 10 | 0.2248 | 0.5238 | 0.3619 | 0.5226 | 0.7534 | 1.1203 | 1.8102 | 3.6311 |

From table 1, we obtain the relationship curves between the dimensionless pore water pressures and various ratio of the horizontal component $k_{xx}$ to vertical component $k_{yy}$ of permeability of the initial soil. Figure 3a expresses the relationships between the pore pressures on the shear plane and on the cutting blade and the ratio of the components $k_{xx}$ to component $k_{yy}$ of the permeability at shear angles 25 degrees and at a cutting angle of 60 degree. Figure 3b express the relationships between the cutting force Fh and the ratio of the components $k_{xx}$ to the component $k_{yy}$ of the permeability for different soil with internal friction angles from 20 ~ 45 degrees at shear angles from 15 ~ 35 degrees.

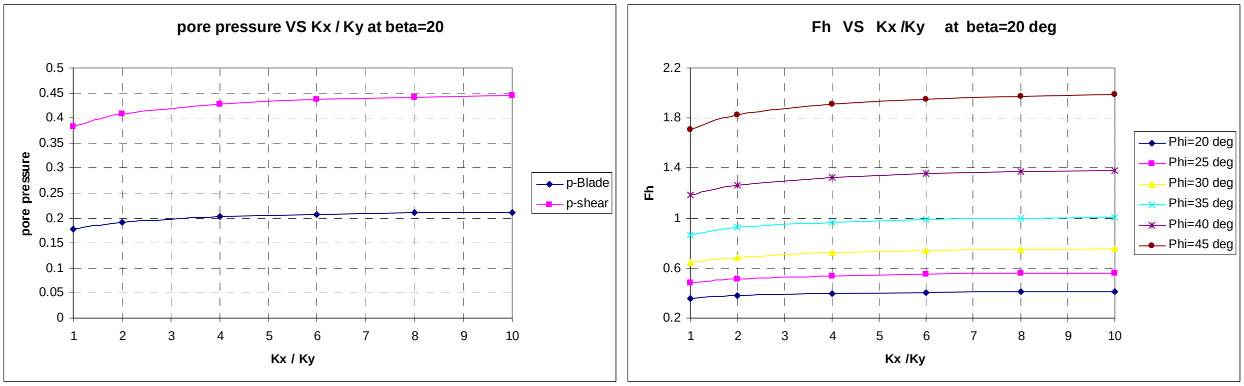


**Figure 3. Cutting forces $F_h$ vs $k_{xx} / k_{yy}$ at α=60 º, β=25 º**

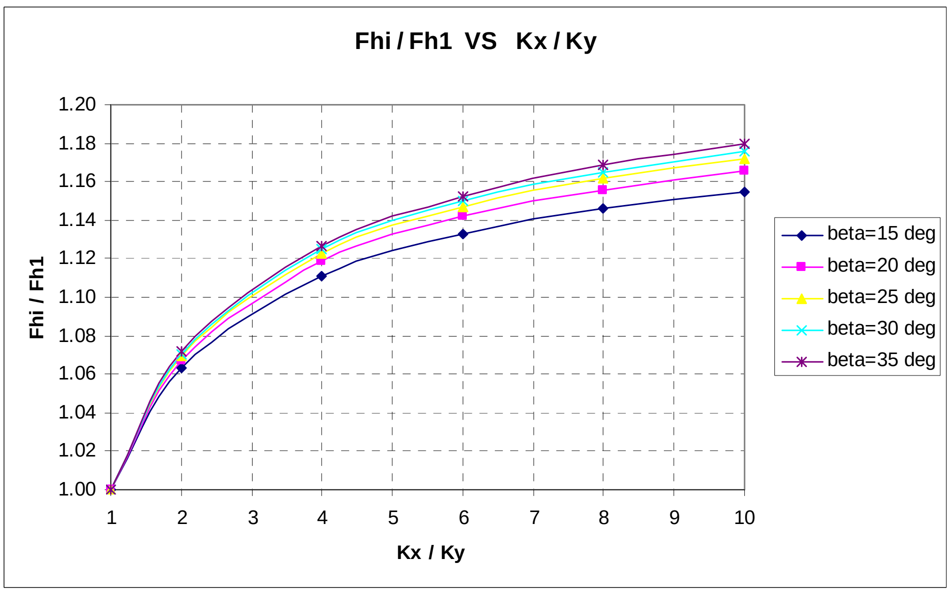


**Figure 4. Ratio of cutting forces $F_h / F_{h1}$ vs $k_{xx} / k_{yy}$ at α=60 ºFigure 5**

Figure 4 expresses the relationship between the ratio of the cutting force from the anisotropic soil to that from the isotropic soil and the ratio of the component $k_{xx}$ to the component $k_{yy}$ of the permeability of the soil. From this figure, when the ratio of the component $k_{xx}$ to component $k_{yy}$ of the permeability of the soil is less than 2, the error of using the calculation results from the isotropic models representing those from the anisotropic model is less than 7 %. However as the anisotropic degree increases, the error will also increases.

Figure 5 expresses the distribution of the excess pore water pressures for the model of the cutting of anisotropic soil while figure 6 expresses the distribution of the excess pore water pressures for the model of the cutting of isotropic soil. After comparing these two figures, it can be found that the distribution of excess pore water pressures for isotropic soil appears vertical ellipse while the distribution for anisotropic soil appears a flatter ellipse and that the values of the excess pore water pressures from the cutting model of anisotropic soil are higher than those from the cutting model of isotropic soil. These show that for anisotropic model pore water flows into shear zones mainly from horizontal direction during soil cutting, and that the resistance of pore water flowing into shear zones is larger than that of the isotropic model.

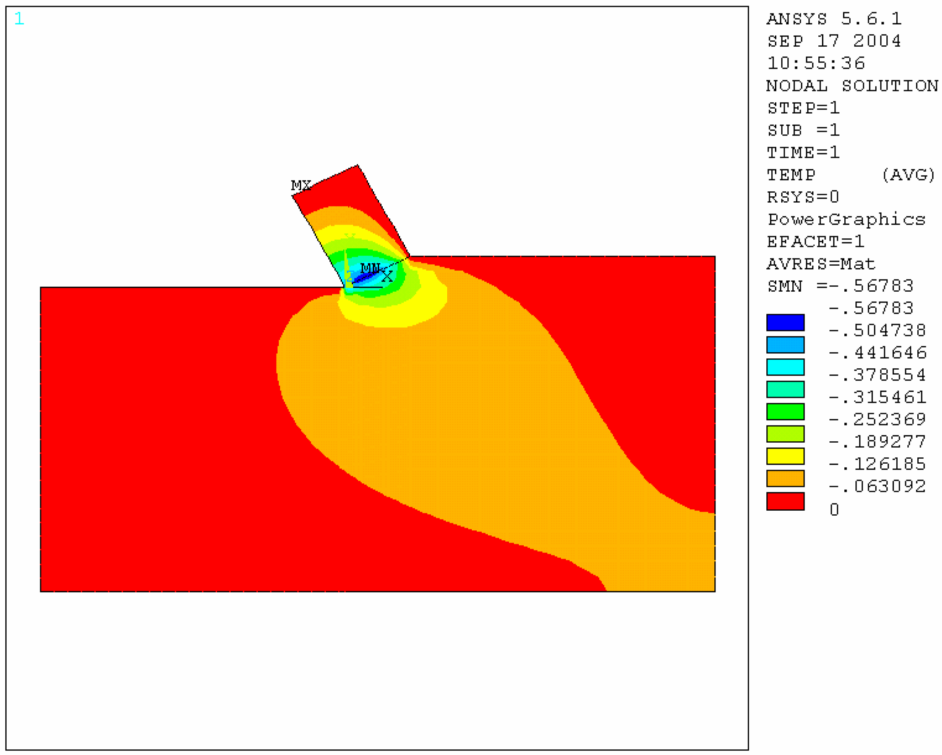


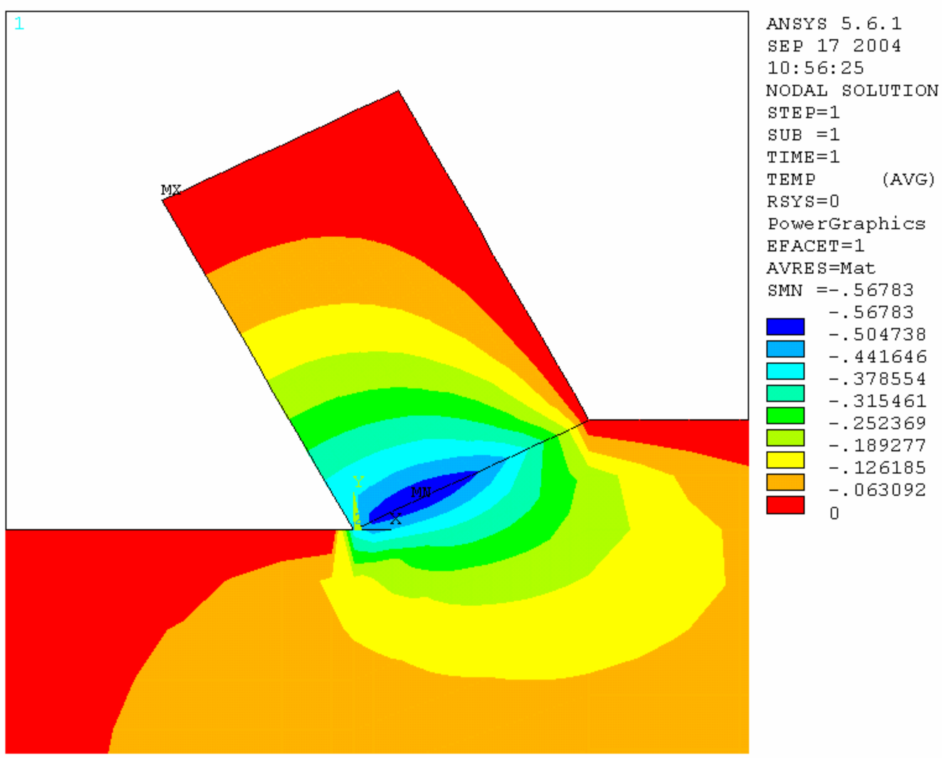


**Figure 6: Distribution of the excess pore water pressures of anisotropic soil model**

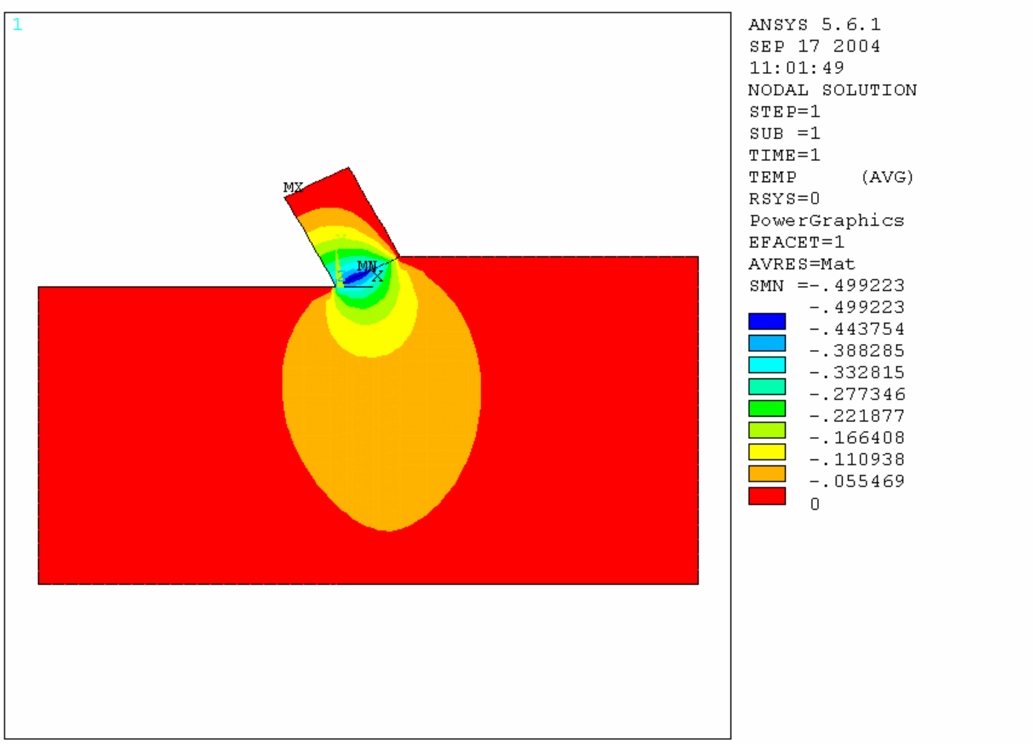


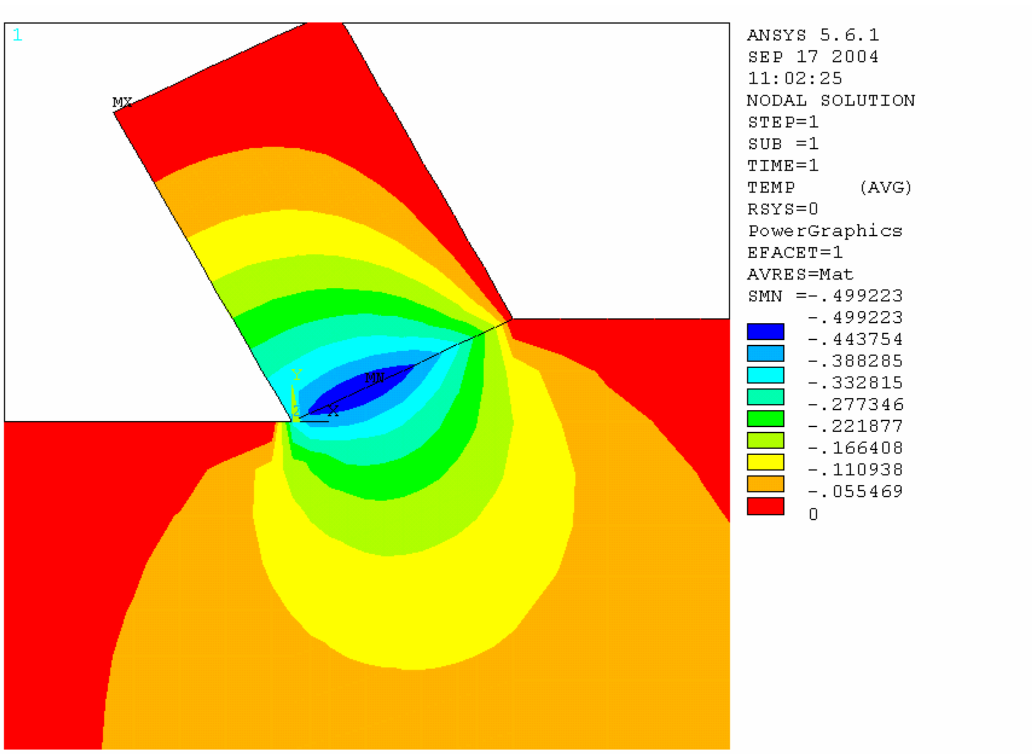


**Figure 7: Distribution of the excess pore water pressures of isotropic soil model**

## CONCLUSIONS

From the analyses above, the following conclusions can be made:

In general speaking, the cutting forces will increase as the ratio of the component $k_{xx}$ to component $k_{yy}$ of the permeability of the soil. When this ration is less than 2, the error of using calculation results from isotropic soil models to represent those from anisotropic soil models is less than 7%. When this ration is 10, the error of using calculation results from isotropic soil models to represent those from anisotropic soil models is less than 20%. In general speaking, the models of the cutting of saturated homogeneous soil are precise enough for the practical situations as is concerned the permeability of the anisotropic soil.

Because of anisotropic property of soil, during the cutting of densely compacted and saturated anisotropic soil, pore water flows into the shear zones mainly in the horizontally direction.

## REFERENCES


Biot, M.A. (1941): “General theory of three dimensional consolidation.” *Journal of Applied Physics*, 12, 155-164

He, Jisong (1997): “Failure Patterns of the 2-D Soil Cutting in Tunneling.” Report number: 97.3 VG.4949, TU Delft, the Netherlands

Kesteren, W. M.G. van, Steeghs, H. J.M.G. and Mastbergen, D.R. (1992): “Pore water behaviour in dredging processes.” *Proceedings WODCON XIV*, Bombay, India

Leussen, W. van and Niewenhuis J.K. (1984): “Soil mechanics aspects of dredging.” *Geotechnique* 34(3), 359-381

Miedema, S.A. (1985A): “Mathematical modeling of the cutting of densely compacted sand under water.” *Journal of Dredging & Port Construction*, July, 22-26

Miedema, S.A. (1985B): “Derivation of the differential equation for sand pore pressures.” *Journal of Dredging & Port Construction, September*, 35

Miedema, S.A. (1987): Calculation of the cutting forces when cutting water saturated sand, basic theory and application for 3-D blade movements and periodically varying velocities in dredging commonly used excavating means, PhD dissertation, Delft University of Technology, the Netherlands

Os, A.G. van (1976): “Behaviour of soil when excavated underwater.” International Course Modern Dredging, The Hague, the Netherlands

Os, A.G. van and Leussen, W. van (1987): “Basic research on cutting forces in saturated sand.” Journal of the Geotechnical Engineering Division, 102, No. GT4, 361-372

Verruijt, A. (1970): *Theory of groundwater flow*, London: Macmillan

Zienkiewicz, O.C. and Taylor, R. L. (1989): *The finite element method*, New York: McGraw-Hill Book Company